

**PRESSURE-DRIVEN STRUCTURAL TRANSITIONS  
IN MOLTEN SALTS**ROMINA RUBERTO,<sup>a</sup> GIORGIO PASTORE,<sup>b\*</sup> AND MARIO P. TOSI<sup>c</sup>

ABSTRACT. Liquid-structure types of molten salts near freezing at standard pressure have been classified on the basis of the relationship between melting entropy  $\Delta S$  and melting volume  $\Delta V$  in correlation with measured values of transport coefficients. Here we report on the evolution of these liquid-structure types under compression, with main attention to  $\text{ZnCl}_2$  and  $\text{AlCl}_3$  for which data from classical molecular dynamics simulations and from diffraction experiments exist.

**1. Introduction**

The behavior of matter under increasingly high pressures and the phase transitions that occur in the pressure-temperature ( $p, T$ ) plane continue to be a theme of high physical interest. Although the present short review will be focused on binary molten-salt systems, we wish to start by recording some of the developments that have taken place in this area from most recent studies. Thus, observations have been reported of a transition to a transparent dense phase of Sodium under pressure [1], which is attributed to interstitial charge localization resulting from  $3p$ - $3d$  band hybridization, and of a pressure-induced metal-to-semiconductor transition in the electrical resistivity of Lithium [2]. Again with regard to the structure of alkali metals at different densities, the coexistence of numerous structural modifications in high-pressure Sodium explains the presence of a marked minimum in its melting curve [3]. Expansion of the heavy liquid alkalis upon heating towards the liquid-gas critical point and dimer formation occur through a reduction of the coordination number rather than through a dilation of the first-neighbor mean distance [4]. Turning to a unique system that combines the properties of a molecular solid and of a magnet [5], the phase behaviors of high-temperature Oxygen [6], the structure of its metallic phase in a pressure transmitting medium [7] and its magnetically ordered states under pressure [8] have been the object of X-ray and neutron diffraction studies. Finally, moving from condensed matter physics towards astrophysics and cosmology, very remarkable recent studies have regarded (i) the mapping of the molecular-to-atomic transition in compressed liquid Hydrogen from first-principles molecular dynamics [9]; (ii) the distillation of Neon-rich drops of Helium through the atmosphere of Jupiter for an interpretation of data from

NASA's Galileo mission [10]; and (iii) the excursus into matter governed by quantum chromodynamics and the transition from a fluid of hadrons to a quark-gluon plasma through collisions between Gold nuclei in the Relativistic Heavy Ion Collider at Brookhaven National Laboratory [11]. Returning to condensed matter physics, we recall that some years ago Angilella et al. [12] gave a short review of phase transitions that take place wholly within the liquid state. Although some attention was also given to computer-simulation data on water, the main focus of their review was on elemental liquids, both quantal (Hydrogen and the two Helium isotopes) and classical (Carbon, Selenium, Sulphur and Phosphorous). Polyatomic molecular liquids under extreme compression have been discussed in later work [13]. In the present paper we give a short review of recent progress concerning liquid-liquid transitions in compressed binary ionic melts, with main attention to the behavior of  $\text{ZnCl}_2$  and  $\text{AlCl}_3$  in the  $(p, T)$  plane as revealed by diffraction experiments [14, 15] and by classical computer simulation studies [16, 17].

## 2. Structural types of ionic melts near the standard freezing point

There is general consensus that all alkali halide melts near their standard freezing point (sfp) form dissociated ionic liquids, with an ionic electrical conductivity of order  $1 - 10 \Omega^{-1} \text{ cm}^{-1}$  and a shear viscosity of order  $1 - 2 \text{ cp}$  (for a review see Rovere and Tosi [18]). These materials, together with some other monovalent metal halides ( $\text{AgCl}$ ,  $\text{TlBr}$ ,  $\text{TlI}$  and  $\text{InCl}$ ) approximately obey the relationship [19]

$$\Delta S = nR \ln 2 + \alpha B_T \Delta V \quad (1)$$

between the entropy change  $\Delta S$  and the volume change  $\Delta V$  on melting, as first proposed by Tallon and Robinson [20]. In Eq. (1)  $n$  is the number of components in a formula unit,  $R$  is the gas constant,  $\alpha$  is the coefficient of thermal expansion, and  $B_T$  is the isothermal bulk modulus. Insofar as the product  $\alpha B_T$  (equal to  $\gamma C_V/V$  where  $\gamma$  is the Gruneisen parameter and  $C_V$  the heat capacity) takes similar values for similar systems in corresponding states, Eq. (1) implies an approximate linear relationship between  $\Delta S$  and the relative volume change  $\Delta V/V$ , extrapolating for  $\Delta V/V \rightarrow 0$  to a constant value of  $n \ln 2$  for  $\Delta S/R$ .

A few other monovalent-metal halides (e.g.  $\text{AgI}$ ,  $\text{AgBr}$  and  $\text{CuCl}$ ) show instead a deficit in  $\Delta S$  relative to the "norm" given by Eq. (1) with  $n = 2$ . This "missing entropy of melting" is taken to reflect a large increase of entropy of the solid below the melting point, due to massive disordering of one of the two atomic lattices (in particular, hot solid  $\text{AgI}$  is the prototypic superionic conductor, the high solid-state electrical conductivity being attributed to strong disorder in the distribution of positions for the silver ions). Superionicity and premelting disorder of the solid, accompanied by a corresponding deficit in the entropy of melting, appears again in several divalent-metal halides (e.g. in  $\text{BaCl}_2$ ,  $\text{SrCl}_2$  and  $\text{SrBr}_2$ ), where the halogen sublattices grow disordered either through a solid-solid phase transition as in  $\text{AgI}$  or through a continuous rapid increase of the ionic conductivity on the approach to melting as in  $\text{AgBr}$  and  $\text{CuCl}$ . There is no doubt, however, that also the melts deriving from a superionic solid conductor are to be regarded as dissociated ionic liquids, so that the phase behavior of all these melts can be expected to be qualitatively similar under pressure. This behavior will be briefly discussed in Section 3 below.

In addition to dissociated ionic liquids, two new types of melts are met among divalent-metal halides. These are the network-structured systems such as  $\text{ZnCl}_2$ ,  $\text{BeF}_2$  and  $\text{BeCl}_2$ , and the molecular systems such as  $\text{HgCl}_2$ ,  $\text{HgBr}_2$  and  $\text{HgI}_2$ . Molecular-type melts are also prominent among trivalent metal halides [21], well known cases being  $\text{AlCl}_3$ ,  $\text{AlBr}_3$ ,  $\text{AlI}_3$  and  $\text{GaCl}_3$ . In both types the electrical conductivity near the sfp is down by several orders of magnitude, and a prepeak reflecting intermediate-range order has often been reported from neutron diffraction experiments and computer simulation studies [22]. These two structural types are nevertheless distinct because of the following differences in behavior: (i) molecular-type melts approximately satisfy the entropy-volume relationship given in Eq. (1), whereas network-type melts of both dihalides and trihalides show a large deficit in the entropy of melting relative to the “norm” [19]; and (ii) the shear viscosity of the molecular-type melts is again in the centipoise range, whereas in the network-type melts its values are up by several orders of magnitude. Both differences can be understood as being the consequence of the fact that in the latter melts the “network” formed by the halogens survives melting at standard pressure, whereas in the former melts the intermediate range order arises from the coexistence of distinct, though strongly interacting, molecular units. We shall see in Section 3 below that this idea also explains the different structural-transition behaviors that have been reported under pressure for the molecular-type  $\text{AlCl}_3$  melt and for the network-type  $\text{ZnCl}_2$  melt.

### 3. Liquid-liquid transitions in compressed molten salts

In the preceding Section we have used thermodynamic and transport properties to classify the structure of ionic melts near the sfp into three main types, representing dissociated ionic liquids, molecular liquids, and network liquids. In this Section we discuss the evolution of these three structural types under compression, with main attention to the appearance of liquid-liquid transitions. We exclude possible changes in the electronic structure under pressure.

We do not expect any liquid-liquid transition in dissociated ionic liquids. One merely expects that, on driving such a liquid to higher pressure and temperature along the melting curve, there should be a gradual pressure-induced change from an open (NaCl-like, say) structure to a closer-packed structure, as short-range interactions become progressively more important relative to the Coulomb interactions. Such structural changes have been demonstrated by Ross and Rogers [23] in hypernettedchain calculations on a model for CsI, showing that the number-number pair distribution function becomes in strongly compressed states quite similar to that of liquid Xenon.

Liquid-liquid transitions driven by pressure have instead been reported for both  $\text{AlCl}_3$ , a molecular liquid that near the sfp mainly consists of  $\text{Al}_2\text{Cl}_6$  dimers formed by two edge-sharing tetrahedra, and  $\text{ZnCl}_2$ , a prototypic network liquid in which interstices in an extended disordered network of Chlorines accommodate the Zinc ions. The main evidence comes from X-ray diffraction studies carried out under pressure along the melting curve [14, 15], to which computer simulation studies in the liquid state have added considerable details [16, 17]. The first observed consequence of increasing pressure on the liquid near the melting curve is to frustrate its intermediate-range order. At higher pressures the liquid-liquid transitions also induce clear signals in the melting curve  $p_m(T)$ : a rapid decrease

in the slope  $dp_m/dT$  for  $\text{AlCl}_3$ , and a sharp singularity for  $\text{ZnCl}_2$  corresponding to the terminal point of the  $\gamma \rightarrow \delta'$  transition in the crystal.

**3.1. Liquid-liquid transition in  $\text{AlCl}_3$ .** A review of the facts established for the structural transition that occurs under pressure in liquid  $\text{AlCl}_3$  has earlier been published in this journal [24]. It was also accompanied by a detailed description of the molecular dynamics simulation method and of the interionic force model adopted for this material. Here we need only summarize the main points of the evidence.

The simulation reproduces the observed character of the melting curve as being a phase transition from a layered crystal into a molecular liquid at low pressure and temperature and into a dissociated ionic liquid at high pressure and temperature. The liquid-liquid transition is traced by a well defined transition line between the two liquid states and clearly has the character of an insulator-to-conductor transition, associated with the crushing of dimers and higher clusters. With regard to the liquid structure, starting at low pressure and elevated temperature from a majority of monomers and dimers with some admixture of higher clusters, the simulations show that after an initial increase in the monomers the liquid structure can no longer be resolved into clusters. At the same time, the main plateau in the Al-Cl coordination number evolves from about four to about six [25]. In addition to these structural signals and, as far as it can be seen, simultaneously with them, there appear two dynamical signals of the liquid-liquid transition: (i) the self-diffusion coefficient of the Al ions overtakes that of the Cl ions as the metal ions become free from their molecular cages, and (ii) there also appears a drastic change in the frequency distribution of the diffusive motions, from a molecular-like to a plasma-like spectrum. The liquid-liquid transition is accompanied by increases in entropy and density, as shown by the negative sign of the slope  $dp_u/dV$  of the transition line.

**3.2. Liquid-liquid transition in  $\text{ZnCl}_2$ .** Liquid  $\text{ZnCl}_2$  near its sfp has drawn much attention in the literature from being the only pure chloride melt that can be brought into a vitreous state by laboratory quenches taking advantage of its relatively low melting point and of its extremely high viscosity. The molecular-dynamics simulations that we have carried out on this melt were again based on a pseudoclassical model for the ion-ion interactions, which incorporated data on the molecular monomer but also involved some adjustments of the Cl-Cl interactions to liquid-state data near the sfp [26]. These adjustments aimed at (i) reproducing the observed structural connectivity of the liquid as defined in terms of predominant corner-sharing *vs* edge-sharing  $\text{ZnCl}_4$  tetrahedra, and (ii) reproducing the magnitude of the measured diffusion coefficients of the two ionic species as functions of temperature at atmospheric pressure. The net effect of these adjustments in the force law was to increase by a relatively low amount the stiffness of the network formed by the Chlorines. The application of the adjusted force law to calculations on molecular monomers and dimers yields excellent agreement with the results of first-principles quantum mechanical calculations.

The exploration of the thermodynamic plane that was performed in Ref. [17] is reported in Fig. 1. The predicted melting curve consists of two separate, essentially linear branches, and is in essentially quantitative agreement with the measurements. The melt near the sfp shows a covalent network structure sustained by a stable random close packing of the Chlorine ions, which accommodates the Zinc ions in essentially tetrahedral holes: this liquid

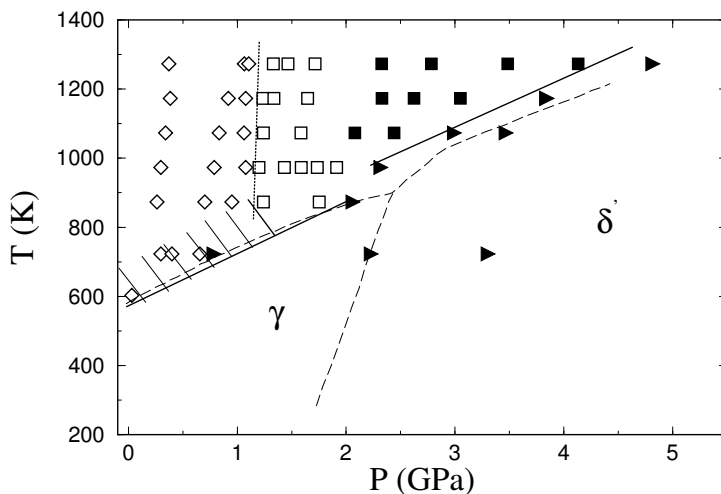


**Figure 1.** Map of the thermodynamic states explored by molecular dynamics simulations in the pressure-temperature plane of  $\text{ZnCl}_2$  and the proposed locations of the melting curve (full lines) and of the liquid-liquid fast-cation transition (dotted line). Intermediate range order of the liquid is visible in the hatched region. The symbols show different structures: network liquid (lozenges), fast-cation liquid (squares), dissociated ionic liquid (filled squares), and solid (filled triangles). The dashed lines report the phase boundaries from the experiments of Brazhkin et al. [15]. Note: 1 GPa = 10 kbar. Redrawn from Ref. [17].

structure is similar to that of the  $\gamma$ - $\text{ZnCl}_2$  phase of the crystal. Again, the intermediate-range order of the melt is frustrated at rather low pressures as one moves along near the lower branch of the melting curve. The network formed by the Cl ions allows relative freedom of diffusion for the Zn ions to set in at lower pressures than those needed for crushing such network into a dissociated ionic liquid. One may thus view the initial stages of the liquid-liquid transition as being, in a sense, analogous to a superionic fast-ion transition in the positive-ion subsystem: the diffusivity of the Zn ions overtakes that of the Cl ions while the covalent network of the latter is still surviving, though slowly changing. The inversion in the magnitudes of the diffusivities of the two ionic species is indeed accompanied by slow increases in their running coordination numbers. Only at higher pressures and temperatures the liquid structure shows clear signals that the transition from a network liquid to a dissociated ionic liquid is complete. One may thus envisage a second line in the liquid phase, that departs from the melting curve in the region where the two branches should meet and separates a “fast-ion conducting liquid” from a dissociated ionic liquid. This second transition line is indicated in Fig. 1 by the transition from empty squares to filled squares.

#### 4. Concluding remarks

In the foregoing we have stressed the differences that arise between the behavior of a molecular-type liquid like  $\text{AlCl}_3$  and that of a network-type liquid like  $\text{ZnCl}_2$  near the melting curve with increasing pressure and temperature. In both cases the final state (barring changes in electronic structure) is that of a dissociated ionic liquid, but the processes with which this state is reached show differences reflecting the structure of the melt near the standard freezing point. Crushing of molecular clusters occurs in the former system, but the latter system goes first through a relative increase in the diffusivity of the metal ions which is then followed by crushing of the network of the halogen ions.

Two interesting lines of further development seem worth mentioning. Whereas the studies that we have reviewed above have both involved compression and increases of density, runs in the opposite direction of decreasing density may yield novel views on the surface structure and the liquid-gas transition in the case of  $\text{ZnCl}_2$ , where the interionic force law that we have developed seems to have fully quantitative value. Secondly, we have already drawn attention elsewhere [17] to the structural behavior of crystalline  $\text{HgI}_2$ , transforming under isobaric heating from a network structure into a molecular structure of linear monomers, and to the lack of microscopic structural studies on its liquid phase. A pseudoclassical model should in this case explicitly include three-body forces, in order to enforce the stability of the linear shape of the monomer and the symmetry breaking in the shape of the dimer. As computers get faster, it is a challenge to look for practicable methods to model materials on the atomic scale, without having to simulate electrons explicitly [27].

#### Acknowledgments

M.P.T. thanks Professor V. E. Kravtsov and the Condensed Matter and Statistical Physics Section of the Abdus Salam International Centre for Theoretical Physics in Trieste for their hospitality.

#### References

- [1] Y. Ma et al., *Nature* **458**,182 (2009).
- [2] T. Matsuoaka and K. Shimizu, *Nature* **458**,186 (2009).
- [3] E. Gregoryanz et al., *Science* **320**, 1054 and 321, 772 (2008).
- [4] R. Winter, W. C. Pilgrim and F. Hensel, *J. Phys.: Condens. Matter* **6**, A245 (1994).
- [5] Yu. A. Freiman and H. J. Jodl, *Phys. Rep.* **408**, 1 (2004).
- [6] L. F. Lundegaard et al., *J. Chem. Phys.* **130**, 164516 (2009).
- [7] G. Weck et al., *Phys. Rev. Lett.* **102**, 255503 (2009).
- [8] S. Klotz et al., *Phys. Rev. Lett.* **104**, 115501 (2010).
- [9] I. Tamblyn and S. A. Boney, *Phys. Rev. Lett.* **104**, 065702 (2010).
- [10] H. F. Wilson and B. Militzer, *Phys. Rev. Lett.* **104**, 121101 (2010).
- [11] C. Gale, *Physics* **3**, 28 (2010).
- [12] G. G. N. Angilella, F. E. Leys, N. H. March and R. Pucci, *Phys. Chem. Liq.* **41**, 211 (2003).
- [13] G. G. N. Angilella and N. H. March, *Phys. Chem. Liq.* **46**, 491 (2008).
- [14] V. V. Brazhkin et al., *IETP Lett.* **82**, 713 (2005).
- [15] V.V. Brazhkin et al., *J. Phys.: Condens. Matter* **19**, 246104 (2007).
- [16] R. Ruberto, G. Pastore and M. P. Tosi, *Phys. Lett. A* **372**, 5215 (2008).
- [17] R. Ruberto, G. Pastore and M. P. Tosi, *Phys. Lett. A* **373**, 1083 (2009).
- [18] M. Rovere and M. P. Tosi, *Rep. Progr. Phys.* **49**, 1001 (1986).

- [19] Z. Akdeniz and M. P. Tosi, *Proc. R. Soc. London A* **437**, 85 (1992).  
[20] J. L. Tallon and W. H. Robinson, *Phys. Lett. A* **87**, 165 (1982).  
[21] M. P. Tosi, D. L. Price and M.-L. Saboungi, *Ann. Rev. Phys. Chem.* **44**, 173 (1993).  
[22] We hasten to add, however, that we know of no structural investigation of the state of short and possible intermediate range order for the mercury halide melts cited in the text. The crystalline structures of these materials at premelting are best viewed as molecular crystals composed of monomeric formula units, and melting yields liquids with very low ionic conductivity and “normal” viscosity. The monomers retain their distinct identities in the gaseous dimers through symmetry breaking arising from relativistic effects (K, J. Donald, M. Hargittai and R. Hoffmann, *Chem. Eur. J.* **15**, 158 (2008)).  
[23] M. Ross and F. J. Rogers, *Phys. Rev. B* **31**, 1463 (1985).  
[24] R. Ruberto, G. Pastore and M. P. Tosi, *Atti Accad. Pelor.* **87**, 1 (2009).  
[25] R. Ruberto, G. Pastore and M. P. Tosi, *Phys. Chem. Liq.* **46**, 548 (2008).  
[26] R. Ruberto, G. Pastore and M. P. Tosi, *Physica B* **405**, 974 (2010).  
[27] See e.g. A. B. Bartok, M. C. Payne, R. Kondor and G. Csanyi, *Phys. Rev. Lett.* **104**, 136403 (2010).

---

<sup>a</sup> Università degli Studi di Messina  
CNISM  
and  
Dipartimento di Fisica  
Contrada Papardo  
98166 Messina, Italy

<sup>b</sup> Università degli Studi di Trieste  
Dipartimento di Fisica  
and  
CNR-IOM DEMOCRITOS National Simulation Center  
Strada Costiera 11  
34151 Trieste, Italy

<sup>c</sup> Scuola Normale Superiore  
Piazza dei Cavalieri 7  
56126 Pisa, Italy

\* To whom correspondence should be addressed | e-mail: pastore@ts.infn.it

Presented 27 May 2010; published online 5 January 2011

© 2011 by the Author(s); licensee *Accademia Peloritana dei Pericolanti*, Messina, Italy. This article is an open access article, licensed under a [Creative Commons Attribution 3.0 Unported License](https://creativecommons.org/licenses/by/3.0/).